JACS
JOURNAL OF THE AMERICAN CHEMICAL SOCIETY

Article

pubs.acs.org/JACS

# From Aggregation-Induced Emission of Au(I)−Thiolate Complexes to Ultrabright Au(0)@Au(I)−Thiolate Core−Shell Nanoclusters

Zhentao Luo,[†] Xun Yuan,[†] Yue Yu,[†] Qingbo Zhang,[‡] David Tai Leong,[†] Jim Yang Lee,[†] and Jianping Xie*,[†]

[†]Department of Chemical and Biomolecular Engineering, National University of Singapore, 10 Kent Ridge Crescent, Singapore 119260

[‡]Department of Chemistry, Rice University, Houston, Texas 77251-1892, United States

Supporting Information

**ABSTRACT:** A fundamental understanding of the luminescence of Au−thiolate nanoclusters (NCs), such as the origin of emission and the size effect in luminescence, is pivotal to the development of efficient synthesis routes for highly luminescent Au NCs. This paper reports an interesting finding of Au(I)−thiolate complexes: strong luminescence emission by the mechanism of aggregation-induced emission (AIE). The AIE property of the complexes was then used to develop a simple one-pot synthesis of highly luminescent Au−thiolate NCs with a quantum yield of ∼15%. Our key strategy was to induce the controlled aggregation of Au(I)−thiolate complexes on in situ generated Au(0) cores to form Au(0)@Au(I)−thiolate core−shell NCs where strong luminescence was generated by the AIE of Au(I)−thiolate complexes on the NC surface. We were able to extend the synthetic strategy to other thiolate ligands with added functionalities (in the form of custom-designed peptides). The discovery (e.g., identifying the source of emission and the size effect in luminescence) and the synthesis protocols in this study can contribute significantly to better understanding of these new luminescence probes and the development of new synthetic routes.

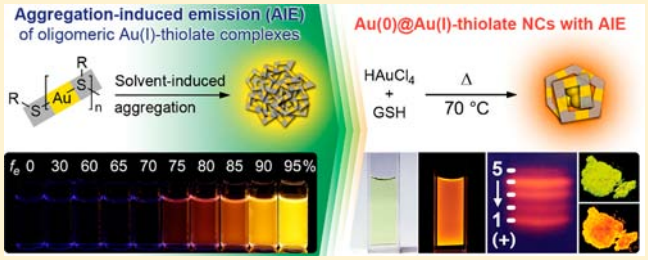


## INTRODUCTION

Thiolate-protected gold nanoclusters (Au−thiolate NCs for short) are ultrasmall (<2 nm) nanoparticles stabilized by thiolate ligands.[1,2] The recent interest in this subgenre of nanoparticles is due to their significance in basic and applied research (e.g., as the missing link between atoms and nanocrystals[1−4] and the utilization of their molecularlike properties such as quantized charging[5−8] and luminescence[9−13] for application developments). The most interesting feature of Au−thiolate NCs is their luminescence properties. Luminescent Au−thiolate NCs, which combine strong luminescence with low toxicity, ultrafine size, and good biocompatibility, are ideal bioimaging and theranostic probes[14−16] only if they can be synthesized by general and convenient methods.

Au−thiolate NCs are commonly prepared bottom-up by the reaction between Au(I)−thiolate complexes and a strong reducing agent, such as sodium borohydride ($NaBH_4$).[17−20] While the resulting Au−thiolate NCs show luminescence in the blue to near-infrared region, their quantum yield (QY) rarely exceeds 0.1%.[1] Recent studies have shown that strongly luminescent Au−thiolate NCs can also be produced by a top-down approach via the decomposition of large Au nanocrystals (>2 nm)[21] or large Au(I)−thiolate complexes (∼120 nm).[22] However, the decomposition kinetics is slow, requiring a very long time for reaction completion [e.g., 2 weeks for the decomposition of large Au(I)−thiolate complexes]. There is also the onerous post-treatment to separate the NCs from incompletely decomposed reaction intermediates.

Understanding the origin of luminescence in Au−thiolate NCs can improve the design and synthesis for strong luminescence. However, several issues fundamental to the luminescence of Au−thiolate NCs, such as the source of emission (whether it is from Au atoms in the core or on the NC surface), the size effect in luminescence, and the critical factors in QY, are still presently not well understood.[1] Since almost all Au−thiolate NCs are formed by the reduction of Au(I)−thiolate complexes, a careful study of Au(I)−thiolate complexes can provide new insights for a better understanding of the luminescence properties of Au−thiolate NCs.

This article is an account of our investigation of Au(I)−thiolate complexes. The most important finding is the discovery of the mechanism of aggregation-induced emission (AIE);[23] that is, nonluminescent oligomeric Au(I)−thiolate complexes can generate very strong luminescence upon aggregation, with intensity and color of the luminescence dependent on the degree of aggregation. The AIE discovery was then used to design highly luminescent Au−thiolate NCs and their synthesis by a facile one-pot procedure. Specifically, these are core−shell-structured Au(0)@Au(I)−thiolate NCs [hereafter referred to

Received: June 25, 2012
Published: September 24, 2012

   dx.doi.org/10.1021/ja306199p | J. Am. Chem. Soc. 2012, 134, 16662−16670

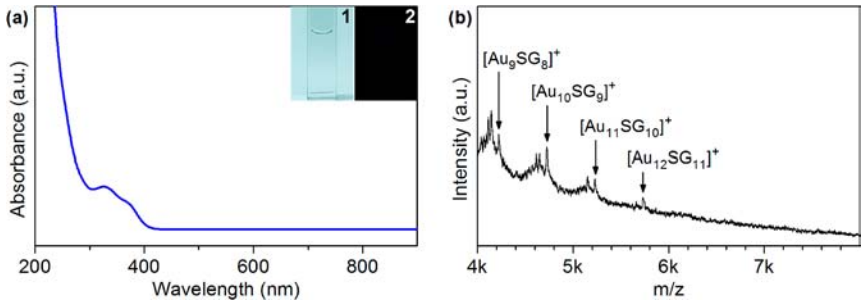


**Figure 1.** (a) UV−vis absorption spectrum and (b) MALDI-TOF mass spectrum of oligomeric Au(I)−thiolate complexes. (Inset) Digital photos of the complexes in water under (1) visible and (2) UV light.

as Au(0)@Au(I)−thiolate NCs] formed by the aggregation of Au(I)−thiolate complexes and in situ generated atomic Au species. The Au NCs synthesized as such have a high content of Au(I)−thiolate complexes in the shell of the core−shell nanostructure, which gives rise to the strong luminescence of the NCs. The versatility and general utility of the procedures was then demonstrated by the synthesis of luminescent Au NCs protected by different types of thiolate ligands.

## EXPERIMENTAL SECTION

**Chemicals.** All chemicals were commercially available and used without further purification. L-Glutathione in the reduced form (GSH) and 2,5-dihydroxybenzoic acid (DHB) were obtained from Sigma−Aldrich. Hydrogen tetrachloroaurate trihydrate ($HAuCl_4 \cdot 3H_2O$) was provided by Alfa Aesar. Custom-designed tripeptides including Glu-Cys-Glu, Ser-Cys-Ser, and His-Cys-His were supplied by GL Biochem Ltd. (Shanghai, China). Ultrapure water (Milli-Q) with a resistivity of 18.2 MΩ was used as the general solvent throughout the study.

**Synthesis of Oligomeric Au(I)−Thiolate Complexes.** Freshly prepared aqueous solutions of $HAuCl_4$ (20 mM, 0.50 mL) and GSH (100 mM, 0.20 mL) were mixed with 4.30 mL of ultrapure water under gentle stirring (500 rpm) at 25 °C for 5 min. A precipitate was formed. NaOH (0.5 M) was then added to the mixture to bring the pH to ∼7.0. The precipitate was dissolved within seconds, and the solution was aged for ∼1 h. The oligomeric Au(I)−thiolate complexes formed as such were used without purification and could be stored at 4 °C for 3 months without any changes.

**Synthesis of Luminescent Au−Thiolate NCs.** Freshly prepared aqueous solutions of $HAuCl_4$ (20 mM, 0.50 mL) and GSH (100 mM, 0.15 mL) were mixed with 4.35 mL of ultrapure water at 25 °C. The reaction mixture was heated to 70 °C under gentle stirring (500 rpm) for 24 h. An aqueous solution of strongly orange-emitting Au NCs was formed. The orange-emitting Au NC solution could be stored at 4 °C for 6 months with negligible changes in their optical properties. The synthesis of luminescent Au NCs protected by other thiolate-containing tripeptides was carried out under similar conditions except for the replacement of GSH by other tripeptides.

**Materials Characterization.** UV−vis absorption and photoluminescence (PL) spectra were recorded by a Shimadzu UV-1800 photospectrometer and a PerkinElmer LS-55 fluorescence spectrometer, respectively. Photoluminescence lifetimes were measured by time-correlated single-photon counting (TCSPC) on a Horiba Jobin Yvon Fluorolog-3 spectrofluorometer with a pulsed light-emitting diode (LED) (344 nm, pulse duration <1 ns) as the excitation source. The size of the aggregates of Au(I)−thiolate complexes was measured by dynamic light scattering (DLS) on a Malvern Zetasizer Nano ZS. Transmission electron microscopy (TEM) images of NCs were taken on a JEOL JEM 2010 microscope operating at 200 kV. Matrix-assisted laser desorption/ionization time-of-flight (MALDI-TOF) mass spectrometry was carried out on a Bruker Daltonics Autoflex II MALDI TOF/TOF system. A Bruker MicroTOF-Q ESI time-of-flight system operating in the negative ion mode (sample injection rate 120 $\mu L \cdot min^{-1}$; capillary voltage 4 kV; nebulizer 1.5 bar; dry gas 4 $L \cdot min^{-1}$ at 160 °C; and $m/z$ 1000−6000) was used for electrospray ionization mass spectrometry (ESI-MS). X-ray photoelectron spectroscopy (XPS) measurements were performed on a VG Escalab MKII spectrometer. The yield of luminescent Au−thiolate NCs based on the Au atoms in the starting mixture was calculated from inductively coupled plasma mass spectrometry (ICP-MS) measurements on an Agilent 7500A. Thermogravimetric analysis (TGA) was conducted on a Shimadzu TGA-60 analyzer under $N_2$ atmosphere (flow rate of 100 $mL \cdot min^{-1}$). Native polyacrylamide gel electrophoresis (PAGE)[3,18,24,25] was carried out on a Bio-Rad Mini-Protean Tetra Cell system using discontinuous gels (1.0 × 83 × 73 mm). Stacking and resolving gels were prepared from 4 and 30 wt % acrylamide monomers, respectively. For analytical gels (10-well), sample solutions (10 $\mu$L of Au NCs with 1.4 mM Au in 6 vol % glycerol) were loaded into the wells of the stacking gel. For preparative gels (5-well), sample solutions (20 $\mu$L of Au NCs with ∼20 mM Au in 6 vol % glycerol) were loaded into the wells. The electrophoresis was allowed to run for ∼2.5 h at a fixed voltage of 200 V at 4 °C.

## RESULTS AND DISCUSSION

**Aggregation-Induced Emission of Au(I)−Thiolate Complexes.** In this study, a natural tripeptide, glutathione (GSH = γ-Glu-Cys-Gly), was used as the model thiolate ligand for the synthesis of oligomeric Au(I)−thiolate complexes. The complexes were formed by mixing aqueous solutions of GSH and $HAuCl_4$ at 25 °C for 5 min, followed by NaOH addition to bring the pH of the mixture to ∼7.0 and aging for ∼1 h. Formation of the complexes involved two steps. The first step was the reduction of Au(III) to Au(I) by GSH,[17,26,27] followed immediately by the coordination of Au(I) to the thiol group to form insoluble aggregates of Au(I)−thiolate complexes. The second step, which was initiated by the addition of NaOH, was the dissolution of the aggregates and the oligomerization of Au(I)−thiolate complexes. The negative charge on the GSH (isoelectric point of pH 2.85)[28] at pH 7.0 imparts good water solubility to the complexes. The resultant reaction mixture was clear and colorless (inset of Figure 1a, item 1) with two distinct


dx.doi.org/10.1021/ja306199p | J. Am. Chem. Soc. 2012, 134, 16662−16670

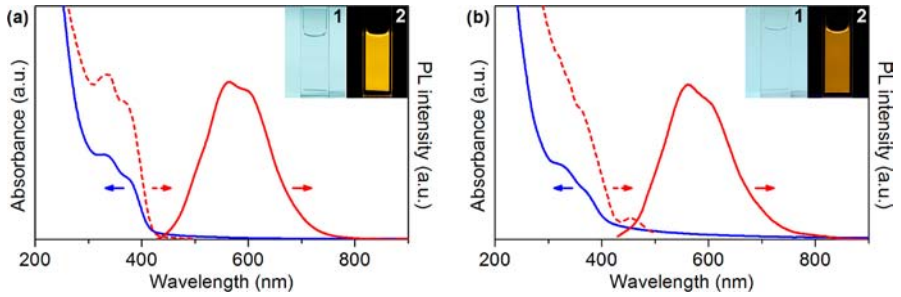


**Figure 2.** UV−vis absorption (solid blue lines), photoemission (solid red lines, $\lambda_{ex}$ = 365 nm), and photoexcitation (dotted red lines, $\lambda_{em}$ = 610 nm) spectra of Au(I)−thiolate complexes aggregated by (a) ethanol (95% ethanol by volume) and (b) $Cd^{2+}$ ions (with $Cd^{2+}$-to-GSH ratio of 1:2). (Insets) Digital photos of aggregated complexes under (1) visible and (2) UV light.

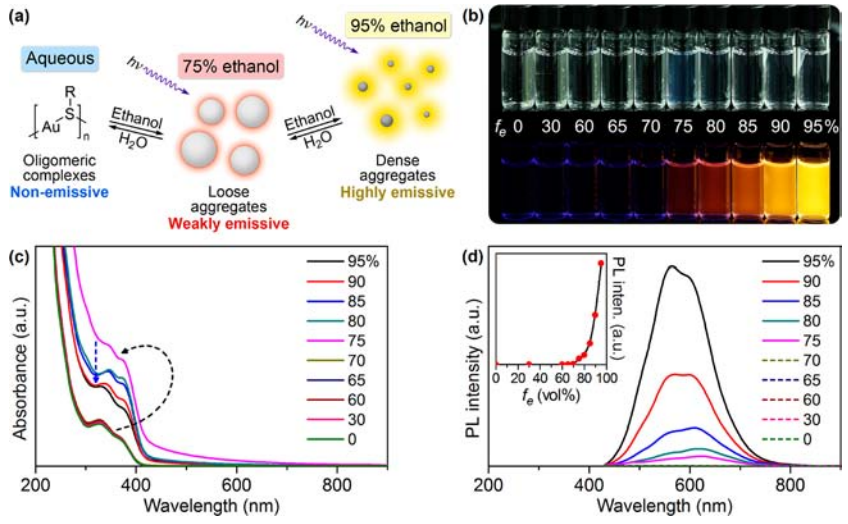


**Figure 3.** (a) Schematic illustration of solvent-induced AIE properties of oligomeric Au(I)−thiolate complexes. (b) Digital photos of Au(I)−thiolate complexes in mixed solvents of ethanol and water with different $f_e$ under visible (top row) and UV (bottom row) light. (c) UV−vis absorption and (d) photoemission spectra of Au(I)−thiolate complexes in mixed solvents with different $f_e$. (Inset) Relationship between the luminescence intensity and $f_e$. The spectra were recorded 30 min after the sample preparation.

absorption peaks at 330 and 375 nm in the UV−vis region (Figure 1a). The locations of these peaks are a good match for the $Au_{10-12}SG_{10-12}$ species reported by Negishi et al.[3] The small size of the Au(I)−thiolate complexes was substantiated by MALDI-TOF mass spectrometry where the largest species in the raw product was $[Au_{12}SG_{11}]^+$ (Figure 1b). Native PAGE (30%) analyses provided yet another line of evidence for the small size of the complexes: there was only one dark band under UV irradiation (Figure S1c, Supporting Information) and the mobility of the band was the same as that of $Au_{10-12}SG_{10-12}$ (Figure S1a, Supporting Information).[3]

The oligomeric Au(I)−thiolate complexes in aqueous solution were not luminescent under UV light (inset of Figure 1a, item 2). However, the complexes upon aggregation generated strong luminescence, as shown in the insets of Figure 2. Such aggregation-induced emission (AIE) phenomenon has recently been observed in luminophore systems involving organic, organometallic, and polymeric luminogens.[23] The aggregation of oligomeric Au(I)−thiolate complexes was induced by two different approaches: solvent-induced aggregation and cation-induced aggregation. The solvent-induced aggregation method made use of a weakly polar solvent, ethanol (dielectric constant of ∼25.3),[29] to destabilize the complexes in water (dielectric constant of ∼80.1).[30] The addition of a high concentration of ethanol (e.g., 95% by volume) in water disrupted the hydration shell of Au(I)−thiolate complexes, resulting in charge neutralization and consequent aggregation of the complexes. The aggregation of Au(I)−thiolate complexes also promoted intra- and intercomplex aurophilic interactions between the closed-shell metal centers [$5d^{10}$ for Au(I)]. The Au(I)···Au(I) interaction is greatly magnified by relativistic effects and has a typical bond energy of 29−46 kJ·mol$^{-1}$ which is comparable to that of a hydrogen bond.[31,32] The formation of aurophilic bonds in turn provided the impetus for aggregation, and denser and more rigid aggregates were formed.

The cation-induced aggregation method, on the other hand, exploited the high affinity of electrostatic and coordination interactions[33] between certain multivalent cations (e.g., $Cd^{2+}$) and the monovalent carboxylic anions (from GSH) in the complexes to form inter- and/or intracomplex cross-links. Besides neutralizing the negative charge on the complexes, the cross-linkers also brought the Au(I)−thiolate complexes closer and facilitated the formation of aurophilic bonds and dense aggregates.

The UV−vis absorption spectra of both solvent-induced (Figure 2a, solid blue line) and cation-induced (Figure 2b, solid blue line) aggregates bear a strong resemblance to the spectrum of oligomeric Au(I)−thiolate complexes (Figure 1a). The stronger background scattering at wavelengths <600 nm was


dx.doi.org/10.1021/ja306199p | J. Am. Chem. Soc. 2012, 134, 16662−16670

due to the larger size of the aggregates. The strong Rayleigh scattering of a red laser pointer beam by a dispersion of the aggregates (Figure S2b,c, Supporting Information) versus no visible Rayleigh scattering by the solution of oligomeric Au(I)−thiolate complexes (Figure S2a, Supporting Information), is another proof of the existence of large aggregates. The photoemission spectra (Figure 2, solid red lines) of the aggregates exhibited two peaks at 565 and 610 nm. The aggregates showed a broad excitation band (Figure 2, dotted red lines) with two shoulder peaks at 330 and 375 nm in correspondence with their two absorption peaks (Figure 2, solid blue lines). The large Stokes shift (>200 nm) suggests that the emission from aggregated Au(I)−thiolate complexes was mainly phosphorescence. This was also supported by photoluminescence lifetime measurements. Analysis of the luminescence decay response confirmed the predominance of microsecond lifetime components in the aggregated Au(I)−thiolate complexes [Figure S3 and Table S1, Supporting Information: 2.93 $\mu$s (85%) and 0.455 $\mu$s (14%) for the ethanol-induced aggregates, 2.41 $\mu$s (79%) and 0.355 $\mu$s (18%) for the $Cd^{2+}$-induced aggregates]. The emission from the aggregates could be attributed to ligand-to-metal charge transfer (LMCT) or ligand-to-metal−metal charge transfer (LMMCT) from the sulfur atom in the thiolate ligands to the Au atoms, and subsequent radiative relaxation, most likely via a metal-centered triplet state.[34−40]

The dependence of luminescence properties on the aggregation degree of Au(I)−thiolate complexes was examined for the aggregates from solvent-induced aggregation. As illustrated in Figure 3a, the aggregation degree was controlled by the polarity of the mixed solvent, which could be varied by the volume fraction of ethanol in the solvent $f_e = vol_{ethanol}/vol_{ethanol+water}$. Increasing $f_e$ increased the aggregation and formed denser and smaller aggregates. Figure 3b (top row) shows that the complex solution was clear and nonluminescent until $f_e$ was 75%, at which time the solution turned cloudy with very weak red emission due to the incipient formation of aggregates. Increasing $f_e$ to 95% reclarified the solution, suggesting the presence of well-dispersed colloids of denser and smaller aggregates, which was also supported by DLS measurements of the complex solutions with $f_e$ from 75% to 95% (Figure S4, Supporting Information). The solution also emitted very strong yellow luminescence (Figure 3b, bottom row).

UV−vis spectroscopy (Figure 3c) was used to follow the aggregation degree of complexes with increasing $f_e$. The clouding of the reaction mixture at 75% $f_e$ also caused a sudden hyperchromic shift (Figure 3c, dotted black arrow) of the UV−vis absorption spectrum due to the large increase in background scattering. When $f_e$ was increased further from 75% to 95%, the formation of smaller and denser aggregates was suggested by hypochromic shifts of the spectrum (Figure 3c, dotted blue arrow). Photoemission spectra (Figure 3d) were also recorded to analyze the emission changes due to variations in aggregation degree. After a $f_e$ value of 75%, the luminescence intensity increased monotonically with the increase in aggregation degree (inset of Figure 3d). The main peak in the emission spectrum also shifted from 630 (red-emitting) to 565 nm (yellow-emitting) with the increase in $f_e$. In addition, the vacuum-dried oligomeric Au(I)−thiolate complexes in the solid state, as an extreme form of dense aggregation, also exhibited strong yellow emission (Figure S5, Supporting Information). The solvent-induced AIE of the oligomeric Au(I)−thiolate complexes was reversible since decreasing $f_e$ could redissolve the aggregates, thereby annulling the AIE mechanism and subsequently quenching the luminescence (see video in Supporting Information).

Some inference about the AIE of Au(I)−thiolate complexes can be made from the above observations, especially the relationship between luminescence intensity and the degree of aggregation: (1) Increasing the degree of aggregation increased the intra- and intercomplex aurophilic Au(I)···Au(I) interactions and consequently the luminescence intensity of the complexes.[31,35,41] (2) Stronger inter- and intracomplex interactions (e.g., van der Waals force and aurophilic interactions) due to aggregation increased the restraints on the intramolecular vibrations and rotations of the complexes; the probability of nonradiative relaxation of the excited states was reduced as a result and this enhanced the luminescence further.[23,42] Hence, dense aggregates generated more intense luminescence because of their stronger aurophilic Au(I)···Au(I) interactions and more restrained molecular vibrations. However, it is still unclear how the increase in aggregation degree led to the observed blue shift in luminescence (Figure 3d). One possible explanation is that, with the increase in aggregation degree, intercomplex aurophilic interactions predominated over intracomplex aurophilic interactions.[43] The longer Au(I)···Au(I) distance in intercomplex aurophilic interactions therefore led to a higher emission energy (or shorter emission wavelength).[35,44]

While the aggregation of Au(I)−thiolate complexes could generate strong luminescence, the aggregates were large and polydispersed and hence easily salted out from the solution. Such propensities limited their usability as practical luminescence probes. However, the discovery of the AIE properties of Au(I)−thiolate complexes has enabled us to develop a novel synthetic route to synthesize highly luminescent Au−thiolate NCs in water.

**Synthesis of Highly Luminescent Au−Thiolate NCs.** The key strategy in our synthesis of highly luminescent Au−thiolate NCs was to condense the Au(I)−thiolate complexes into a compact shell on an in situ generated Au(0) core. The core−shell construction and the small size of the NCs imparted stability and good solubility in water due to the charge and steric stabilization effects of the GSH ligands in the shell. GSH was the reducing-cum-protecting agent in the synthesis, and reaction temperature was used to vary its dual functionality. Protection of Au(I)−thiolate complexes from reduction in the process and control of their aggregation on the Au(0) surface were crucial to the formation of highly luminescent Au−thiolate NCs. In a typical synthesis, aqueous solutions of $HAuCl_4$ and GSH (thiolate ligands) were mixed and allowed to react under gentle stirring at an elevated temperature of 70 °C for 24 h. The reaction mixture changed from yellow to colorless within minutes and then turned to light yellow slowly. The typical yield of luminescent Au−thiolate NCs based on the amount of Au atoms in the starting mixture was ∼90% according to ICP-MS measurements.

Figure 4 is a postulation of the formation of highly luminescent Au−thiolate NCs in three stages. The first stage was the reduction of Au(III) to Au(I) by the thiol group of GSH [or the disulfide group from the resultant oxidized GSH (GSSG)[17,26,27]]; and the immediate coordination of Au(I): to the thiol group of GSH, to form Au(I)−thiolate complexes, or to other functional groups in GSH (e.g., the carboxyl groups) or small anions in the solution (e.g., chloride), to form Au(I)−


dx.doi.org/10.1021/ja306199p | J. Am. Chem. Soc. 2012, 134, 16662−16670

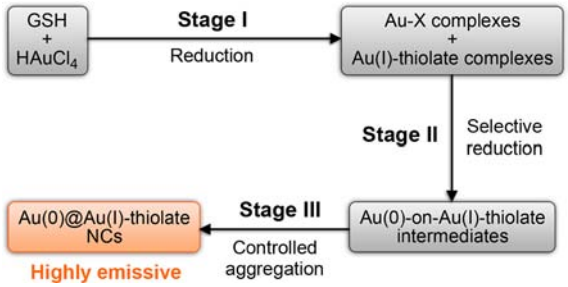


**Figure 4.** Schematic of synthesis of highly luminescent Au(0)@Au(I)−thiolate NCs. X in the Au(I)−X complexes can be any nonthiolate functional group in the reaction mixture.

X complexes (X represents any nonthiolate ligand; Figure 4). The second stage was the selective reduction of Au(I)−X complexes to Au(0) atoms and subsequent sequestration of the Au(0) species by Au(I)−thiolate complexes due to the high affinity between Au(0) atoms and Au(I).[45] Au(0)-on-Au(I)−thiolate intermediates were formed as a result (Figure 4). The reduction of Au(I)−X complexes to Au(0) by the disulfide group of the resultant GSSG (see Figure S6 and detailed discussion in Supporting Information) was made more facile by the favorable reduction kinetics at the elevated temperature of 70 °C. The selectivity of Au(I)−X complexes over Au(I)−thiolate complexes in reduction could be explained by the more positive redox potentials of the former, a consequence of the weaker binding [between Au(I) and X] in Au(I)−X than in Au(I)−thiolate. The third stage was the slow aggregation of Au(0)-on-Au(I)−thiolate intermediates by collision and fusion of Au(0) atoms into a Au(0) core and Au(I)−thiolate complex shell structure. The Au(0)@Au(I)−thiolate NCs synthesized as such had a high content of compact aggregates of Au(I)−thiolate complexes in the shell of the core−shell nanostructure. Very strong luminescence was emitted by the AIE of Au(I)−thiolate complexes condensed in the shell (Figure 4).

Figure 5a shows that the size of the as-synthesized Au(0)@Au(I)−thiolate NCs was below 2 nm. The Au NCs were light-yellow in solution and bright-yellow in the dry state under visible light (inset of Figure 5b, item 1). They emitted intense orange luminescence in both solution and solid state under UV light (inset of Figure 5b, item 2). The NCs displayed excellent stability, including storage in water at room temperature (25 °C; Figure S7a, Supporting Information) and elevated temperature (80 °C; Figure S7b, Supporting Information), in solutions of high salt concentration (e.g., 1 M NaCl; Figure S7c, Supporting Information), and in common buffer solutions [e.g., 40 mM HEPES buffer (pH 7); Figure S7d, Supporting Information]. The luminescence intensity changes were less than 30% even after prolonged storage (7−24 days). The unique structure of these luminescent Au NCs was first suggested by their UV−vis absorption spectrum (Figure 5b, solid blue line), which shows an onset at 500 nm and a shoulder peak at ∼400 nm. Neither surface plasma resonance (SPR at ∼520 nm is typical for spherical nanocrystals larger than 2 nm)[2] nor molecularlike absorption of conventional thiolate-protected Au NCs (peaks at >500 nm for Au−thiolate NCs with more than 15 Au atoms)[3,24,46,47] was detected. The QY of the luminescent Au NCs calibrated with fluorescein was ∼15%, which is orders of magnitude higher than the QY of the reported Au−thiolate NCs (typically 0.001−0.1%).[1] The photoemission spectrum (Figure 5b, solid red line) shows a main peak at 610 nm with a shoulder peak at 565 nm, which correspond with the two emission peaks in the spectrum of the aggregated complexes (Figure 2a, solid red line). Similar to the aggregated complexes (Figure 2a, dotted red lines), the luminescent Au NCs also showed a broad excitation band (Figure 5b, dotted red line) and a large Stokes shift (>200 nm). The microsecond-scale lifetime [1.99 $\mu$s (61%), 0.536 $\mu$s (29%), and 0.144 $\mu$s (8.9%)] of the luminescent Au NCs (Table S1 and Figure S3c, Supporting Information) were also similar to the lifetimes of the aggregated complexes (Figure S3a,b, Supporting Information). The similarity between the NCs and aggregated complexes in terms of luminescence lifetime and spectral features suggests that the emission from Au NCs was derived from the AIE of Au(I)−thiolate complexes on the NC surface.

The high content of Au(I)−thiolate complexes in the luminescent Au NCs was confirmed by XPS and TGA analyses. The XPS spectra in Figure 6a show that the oxidation state of Au in the luminescent Au NCs (black line) was between that of Au(I)−thiolate complexes (red line) and large Au(0) nanocrystals (blue line). The Au 4f spectrum of the luminescent Au NCs was then deconvoluted into Au(I) and Au(0) components with binding energies of 84.3 and 83.7 eV, respectively. The Au(I) content determined as such was found to constitute ∼75% of all Au atoms in the luminescent Au NCs. The thiolate-to-Au ratio in luminescent Au NCs was estimated by TGA. As shown in Figure 6b, GSH contributed ∼56% of the luminescent Au NCs by weight, which can be translated into a thiolate-to-Au ratio of 0.84:1. This value is significantly higher than that of conventional Au−thiolate NCs with more than 15 Au atoms (see the inset of Figure 6b for the thiolate-to-Au ratios of some known Au−thiolate NCs).[1,3,24,48−50] It is, however, close to 1:1

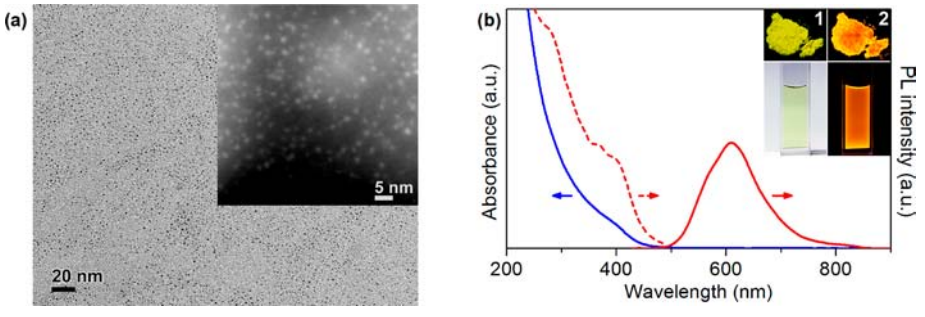


**Figure 5.** (a) TEM and STEM (inset) images of the luminescent Au NCs. (b) UV−vis absorption (solid blue line), photoemission (solid red line, $\lambda_{ex}$ = 365 nm), and photoexcitation (dotted red line, $\lambda_{em}$ = 610) spectra of the luminescent Au NCs. (Insets) Digital photos of luminescent Au NCs in the solid state (top row) and in water (bottom row) under (1) visible and (2) UV light.


dx.doi.org/10.1021/ja306199p | J. Am. Chem. Soc. 2012, 134, 16662−16670

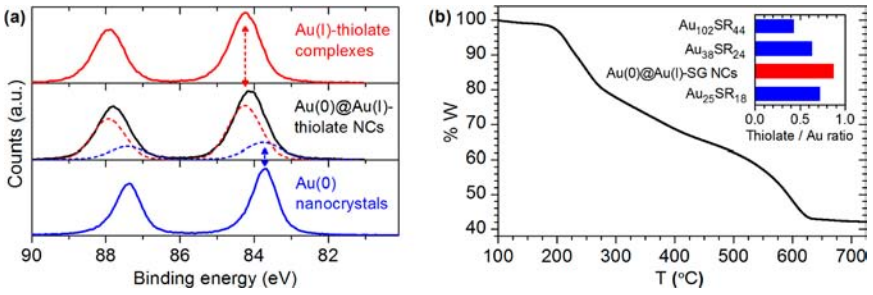


**Figure 6.** (a) Au 4f XPS spectra of Au(I)−thiolate complexes (red line, prepared by mixing GSH and $HAuCl_4$ at room temperature), as-synthesized luminescent Au(0)@Au(I)−thiolate NCs (black line), and large Au(0) nanocrystals (blue line, > 3 nm, prepared by $NaBH_4$ reduction of $HAuCl_4$ without any protecting agent). (b) TGA spectrum of as-synthesized Au(0)@Au(I)−thiolate NCs. (Inset) Thiolate-to-Au ratios of Au(0)@Au(I)−thiolate NCs and three conventional Au−thiolate NCs ($Au_{102}SR_{44}$, $Au_{38}SR_{24}$, and $Au_{25}SR_{18}$).

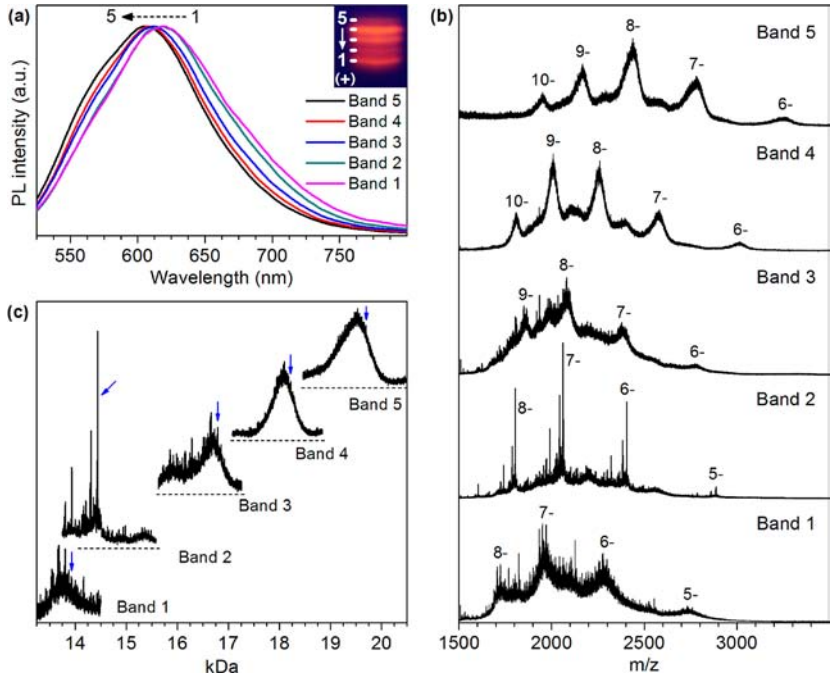


**Figure 7.** (a) Photoemission spectra ($\lambda_{ex}$ = 365 nm) of luminescent Au NCs separated from bands 1−5 in the native PAGE gel (30%). (Inset) Digital photo of the PAGE bands of Au NCs under UV light. All bands moved from the negative to the positive electrode (+), with band 1 showing the highest mobility. (b) ESI mass spectra and (c) corresponding deconvoluted mass spectra of Au NCs harvested from bands 1−5 in the PAGE gel. The arrows in panel c indicate the peaks that have been assigned molecular formulas to represent the size of Au NCs in each band.

thiolate-to-Au ratio reported for many oligomeric or polymeric Au(I)−thiolate complexes.[34,51,52] The high Au(I) content and high thiolate-to-Au ratio are indications of a high content of Au(I)−thiolate complexes in our luminescent Au NCs.

The size of the luminescent Au NCs was further characterized by PAGE analysis and ESI-MS. The native PAGE (30%) analysis of luminescent Au NCs revealed five closely spaced luminescent bands under UV light (inset of Figure 7a), indicating that our luminescent Au NCs were a mixture of NCs with minor differences in size. The mobility of band 1 was similar to that reported for $Au_{33-39}SG_{22-24}$ NCs (see Figure S1 in Supporting Information for detailed analysis),[3] and hence the luminescent NCs were relatively large in size (the size increases from band 1 to band 5). ESI-MS was then used to determine the molecular formula of the NCs in each band. ESI is a soft ionization technique that can be used to determine the NC formula by analyzing the intact NC mass.[1,53,54] The NC bands were individually cut from four preparative gels, added with 5 mL of ultrapure water at 4 °C to allow the NCs in the gels to diffuse out. Twelve hours later, the gel lumps were removed by use of syringe filters (0.45 $\mu$m pore size) and the resulting samples were purified by ultrafiltration (3000 Da molecular weight cut off) and suspended in 500 $\mu$L of ultrapure water for ESI-MS measurement. The ESI mass spectra of the bands (Figure 7b) show a series of multiply charged anions, which can be deconvoluted into the corresponding mass spectra of the uncharged Au NCs (Figure 7c). Due to the uncertainty in fragmentation of the GSH ligand during synthesis and ESI-MS testing, we could not find the molecular formulas of intact or fragmented Au NCs that perfectly match the obtained mass spectra. However, for the intense peaks (e.g., the most intense peak of band 2), we could assign molecular formulas on the basis of their well-defined isotope distributions (see Figure S8 in Supporting Information for detailed analysis). For the less intense peaks, we could estimate their formulas from their mass difference from the assigned peak of band 2. Hence, major peaks (indicated by arrows in Figure 7c) of the Au NCs from bands 1−5 were


dx.doi.org/10.1021/ja306199p | J. Am. Chem. Soc. 2012, 134, 16662−16670

chosen to represent the sizes of the NCs in the corresponding bands, and they could be assigned as $Au_{29}SG_{27}$, $Au_{30}SG_{28}$, $Au_{36}SG_{32}$, $Au_{39}SG_{35}$, and $Au_{43}SG_{37}$, respectively. The ESI-MS measurements confirmed (1) the relatively large size of our luminescent NCs (>29 Au atoms) and (2) a uniquely high thiolate-to-Au ratio (~0.9:1) as compared to that of conventional Au−thiolate NCs with similar numbers of Au atoms.

The size effect of Au−thiolate NCs on emission wavelength was evaluated by analyzing the photoemission spectra (Figure 7a) of Au NCs of different sizes (harvested from the PAGE gel as bands 1−5 in Figure 7a, inset). Contrary to the prediction from the Jellium model where larger-sized NCs should emit longer wavelengths,[55] the main emission peak of our luminescent Au NCs was blue-shifted from 620 to 605 nm with increasing their size (from bands 1−5). This observation is, however, consistent with the AIE properties of aggregated complexes shown in Figure 3d, where denser aggregates emitted at shorter wavelengths (vide infra). Larger Au NCs with a denser aggregation of complexes in their shell should therefore emit at shorter wavelengths if the AIE was the principal source of emission. The experimental size−emission wavelength relationship is therefore an indirect proof of the proposed Au(0)@Au(I)−thiolate NCs structure and the AIE properties of the shell as the origin of luminescence.

The unique optical properties (absorption and luminescence; Figures 5b and 7a) and compositions (Figures 6 and 7b,c) of luminescent Au NCs suggest a different structure from the conventional Au−thiolate NCs (e.g., $Au_{102}SR_{44}$, $Au_{38}SR_{24}$, and $Au_{25}SR_{18}$).[48−50] As illustrated in Figure 8, the Au(I)−thiolate complexes in the shell of our luminescent Au NCs (item ii) were oligomers and very unlike the short Au(I)−thiolate motifs

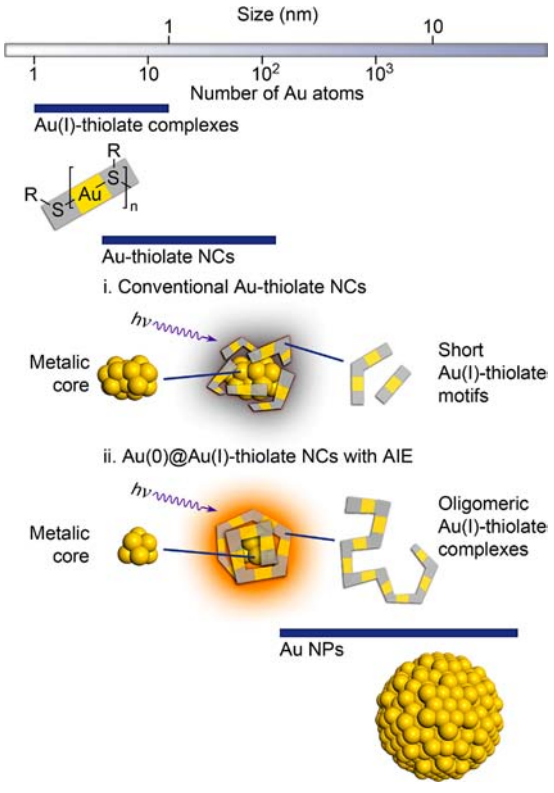


**Figure 8.** Schematic illustration of the structures of (ii) our luminescent Au NCs with AIE and (i) conventional Au−thiolate NCs with short Au(I)−thiolate motifs.

[mono- or dimeric Au(I)−thiolate complexes] that populate the surface of conventional Au−thiolate NCs (item i).[56] The presence of oligomeric Au(I)−thiolate complexes in our NCs was suggested by separate and independent measurements. As shown by our ESI-MS analysis (Figure 7b,c), the overall size of our luminescent Au NCs was relatively large (>29 Au atoms) and the thiolate-to-Au ratio (~0.9:1) was much higher than that of conventional Au−thiolate NCs with a similar number of Au atoms (XPS and TGA analyses in Figure 6). On the other hand, the metallic Au(0) core of our luminescent Au NCs could be smaller than that in the conventional Au−thiolate NCs with similar overall sizes. This was suggested by the large energy gap (~400 nm) in the UV−vis spectrum (Figure 5b). Hence, the thiolate-to-Au ratio for the Au(I)−thiolate complexes in the shell of our luminescent NCs should be close to 1:1, and oligomeric Au(I)−thiolate complexes are the most likely complex species there. However, it is important to note that the detailed structure of the luminescent Au NCs can only be revealed by total structure determination based on the X-ray crystallographic analysis of single crystals of the Au NCs, which is difficult to perform at the moment.

Reaction temperature and GSH-to-Au ratio were identified as the most critical factors in the synthesis of highly luminescent Au NCs. The optimal reaction temperature was ~70 °C, where sufficient Au(I)−X complexes could be reduced to Au(0) atoms while the Au(I)−thiolate complexes were left largely unaffected. The in situ generated Au(0) atoms were sequestered by the Au(I)−thiolate complexes and slowly induced aggregation of the resultant Au(0)-on-Au(I)−thiolate intermediates into Au(0)@Au(I)−thiolate NCs. Both the generation of Au(0) atoms [from the reduction of Au(I)−X complexes] and the preservation of Au(I)−thiolate complexes were important to a successful synthesis. Control experiments carried out at lower reaction temperatures (e.g., 25 °C) formed only large aggregates of insoluble Au(I)−thiolate complexes (Figure S9, Supporting Information). Insufficient reduction of the Au(I)−X complexes at low temperature led to the formation of insoluble Au(I)−thiolate complex aggregates. Another control experiment using a strong reducing agent, $NaBH_4$, produced only a reddish-brown nonluminescent dispersion of Au NCs (Figure S10, Supporting Information). The strong reducing agent $NaBH_4$ was able to decompose Au(I)−thiolate complexes reductively into Au NCs. The content of Au(I)−thiolate complexes in the resulting Au NCs was too low to generate any detectable luminescence (Figure S10, Supporting Information).

The GSH-to-Au ratio was another critical synthesis parameter. Control experiments were also carried out with GSH-to-Au ratios of 0.5:1, 1.5:1 and 2:1. As shown in Figure S11 in Supporting Information, the optimized GSH-to-Au ratio of 1.5:1 was effective in producing luminescent Au NCs. A higher GSH-to-Au ratio (2:1) produced large Au(I)−thiolate complex aggregates, while lower ratios (0.5:1) only formed large Au nanocrystals without any luminescence. The GSH-to-Au ratio of 1.5:1 provided a good balance between the amounts of Au(I)−thiolate complexes and Au(I)−X complexes so that the in situ reduction of the latter generated Au(0) atoms for the aggregation of Au(I)−thiolate complexes into a compact shell of the core−shell structure [Au(0)@Au(I)−thiolate NCs].

**General Utility of the Synthesis Method.** The synthesis method presented above is scalable (e.g., to 100 mL; Figure S12, Supporting Information). It is also suitable for the preparation of luminescent Au NCs protected by other thiolate


dx.doi.org/10.1021/ja306199p | J. Am. Chem. Soc. 2012, 134, 16662−16670

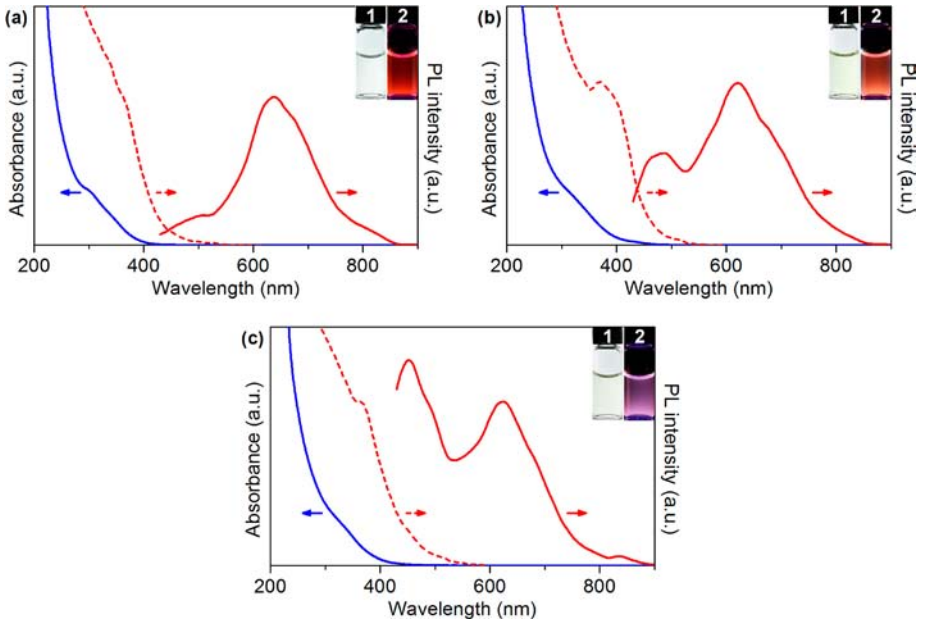


**Figure 9.** UV−vis absorption (solid blue lines), photoexcitation (dotted red lines) and photoemission (solid red lines) spectra of luminescent Au NCs synthesized by custom-designed tripeptides: (a) Glu-Cys-Glu, (b) Ser-Cys-Ser, and (c) His-Cys-His. The excitation spectra were measured at $\lambda_{em}$ = (a) 640, (b) 620, and (c) 625 nm, and the emission spectra were measured at $\lambda_{ex}$ = 365 nm. (Insets) Digital photos of the corresponding NCs under (1) visible and (2) UV light.

ligands, as demonstrated by the following examples. In one experiment, GSH was replaced by other custom-designed tripeptides with the general formula Am-Cys-Am, where Am is an amino acid residue with a desired functional group. The cysteine residue in the middle of the tripeptide is crucial to the synthesis as the provider of the thiolate ligand to generate Au(I)−thiolate complexes. We tested three types of amino acid residues for the Am position: (a) glutamic acid with a carboxyl side group, (b) serine with a hydroxyl side group, and (c) histidine with an imidazole side group. All of the custom-designed tripeptides formed luminescent Au NCs with an emission peak at ∼610 nm, as shown in Figure 9. Hence by use of peptides with a customized length and sequence, highly luminescent Au NCs with the desired surface functionalities can be prepared by our method.

## CONCLUSIONS

In summary, an interesting aggregation-induced emission (AIE) property was discovered in the Au(I)−thiolate complex system. Nonluminescent oligomeric Au(I)−thiolate complexes were found to emit strong luminescence after dense aggregation by either a solvent-induced or cation-induced method. The intensity and color of the luminescence were largely determined by the degree of aggregation. On the basis of this discovery, a simple one-pot synthesis for highly luminescent Au−thiolate NCs was developed with a common thiolate ligand, glutathione, as the reducing-cum-protecting agent. The Au−thiolate NCs fabricated as such had a Au(0)@Au(I)−thiolate core−shell structure formed by the controlled aggregation of Au(I)−thiolate complexes on in situ generated Au(0) cores. High QY (∼15%), large Stokes shift (>200 nm), and the combination of ultrafine size, low toxicity, and good biocompatibility make these luminescent Au−thiolate NCs highly effective as luminescence probes in various biosettings. This facile synthesis method is scalable and can be applied to the preparation of luminescent Au NCs protected by other thiolate ligands.

## ASSOCIATED CONTENT

### Supporting Information

Twelve figures showing native PAGE (30%) analyses of oligomeric Au(I)−thiolate complexes and Au(0)@Au(I)−thiolate NCs, Rayleigh scattering of oligomeric Au(I)−thiolate complexes and aggregated complexes, PL decay profiles, DLS measurements, digital photos of Au(I)−thiolate complexes in the solid state, ESI-MS analysis of the reaction solution of as-synthesized luminescent Au NCs, stability study, detailed analyses of the ESI mass spectra of the Au NCs from band 2, characterizations of products from control experiments, and digital photos from the synthesis of Au(0)@Au(I)−thiolate NCs in a 250 mL flask; one table summarizing lifetimes of aggregated Au(I)−SG complexes and as-synthesized luminescent Au NCs; and one video on the reversibility of solvent-induced AIE of Au(I)−thiolate complexes. This material is available free of charge via the Internet at http://pubs.acs.org.

## AUTHOR INFORMATION

### Corresponding Author

chexiej@nus.edu.sg

### Notes

The authors declare no competing financial interest.

## ACKNOWLEDGMENTS

This work was financially supported by the Ministry of Education, Singapore, under Grants R-279-000-295-133 and R-279-000-327-112.

## REFERENCES

(1) Jin, R. *Nanoscale* **2010**, *2*, 343.
(2) Zhang, Q.; Xie, J.; Yu, Y.; Lee, J. Y. *Nanoscale* **2010**, *2*, 1962.

(3) Negishi, Y.; Nobusada, K.; Tsukuda, T. *J. Am. Chem. Soc.* **2005**, *127*, 5261.
(4) Cademartiri, L.; Kitaev, V. *Nanoscale* **2011**, *3*, 3435.
(5) Bakr, O. M.; Amendola, V.; Aikens, C. M.; Wenseleers, W.; Li, R.; Dal Negro, L.; Schatz, G. C.; Stellacci, F. *Angew. Chem., Int. Ed.* **2009**, *48*, 5921.
(6) Chen, S.; Ingram, R. S.; Hostetler, M. J.; Pietron, J. J.; Murray, R. W.; Schaaff, T. G.; Khoury, J. T.; Alvarez, M. M.; Whetten, R. L. *Science* **1998**, *280*, 2098.
(7) Laaksonen, T.; Ruiz, V.; Liljeroth, P.; Quinn, B. M. *Chem. Soc. Rev.* **2008**, *37*, 1836.
(8) Murray, R. W. *Chem. Rev.* **2008**, *108*, 2688.
(9) Choi, S.; Dickson, R. M.; Lee, J.-K.; Yu, J. *Photochem. Photobiol. Sci.* **2012**, *11*, 274.
(10) Xie, J.; Zheng, Y.; Ying, J. Y. *J. Am. Chem. Soc.* **2009**, *131*, 888.
(11) Wu, Z.; Jin, R. *Nano Lett.* **2010**, *10*, 2568.
(12) Yuan, X.; Luo, Z.; Zhang, Q.; Zhang, X.; Zheng, Y.; Lee, J. Y.; Xie, J. *ACS Nano* **2011**, *5*, 8800.
(13) Negishi, Y.; Tsukuda, T. *Chem. Phys. Lett.* **2004**, *383*, 161.
(14) Baker, M. *Nat. Methods* **2010**, *7*, 957.
(15) Shang, L.; Dong, S.; Nienhaus, G. U. *Nano Today* **2011**, *6*, 401.
(16) Jin, L.; Shang, L.; Guo, S.; Fang, Y.; Wen, D.; Wang, L.; Yin, J.; Dong, S. *Biosens. Bioelectron.* **2011**, *26*, 1965.
(17) Alvarez, M. M.; Khoury, J. T.; Schaaff, T. G.; Shafigullin, M.; Vezmar, I.; Whetten, R. L. *Chem. Phys. Lett.* **1997**, *266*, 91.
(18) Negishi, Y.; Takasugi, Y.; Sato, S.; Yao, H.; Kimura, K.; Tsukuda, T. *J. Am. Chem. Soc.* **2004**, *126*, 6518.
(19) Zhu, M.; Lanni, E.; Garg, N.; Bier, M. E.; Jin, R. *J. Am. Chem. Soc.* **2008**, *130*, 1138.
(20) Templeton, A. C.; Wuelfing, W. P.; Murray, R. W. *Acc. Chem. Res.* **2000**, *33*, 27.
(21) Huang, C.-C.; Yang, Z.; Lee, K.-H.; Chang, H.-T. *Angew. Chem., Int. Ed.* **2007**, *46*, 6824.
(22) Zhou, C.; Sun, C.; Yu, M.; Qin, Y.; Wang, J.; Kim, M.; Zheng, J. *J. Phys. Chem. C* **2010**, *114*, 7727.
(23) Hong, Y.; Lam, J. W. Y.; Tang, B. Z. *Chem. Soc. Rev.* **2011**, *40*, 5361.
(24) Kimura, K.; Sugimoto, N.; Sato, S.; Yao, H.; Negishi, Y.; Tsukuda, T. *J. Phys. Chem. C* **2009**, *113*, 14076.
(25) Schaaff, T. G.; Knight, G.; Shafigullin, M. N.; Borkman, R. F.; Whetten, R. L. *J. Phys. Chem. B* **1998**, *102*, 10643.
(26) Shaw, C. F.; Cancro, M. P.; Witkiewicz, P. L.; Eldridge, J. E. *Inorg. Chem.* **1980**, *19*, 3198.
(27) Witkiewicz, P. L.; Shaw, C. F. *J. Chem. Soc., Chem. Commun.* **1981**, 1111.
(28) Pirie, N. W.; Pinhey, K. G. *J. Biol. Chem.* **1929**, *84*, 321.
(29) Hassion, F. X.; Cole, R. H. *J. Chem. Phys.* **1955**, *23*, 1756.
(30) Archer, D. G.; Wang, P. *J. Phys. Chem. Ref. Data* **1990**, *19*, 371.
(31) Schmidbaur, H. *Chem. Soc. Rev.* **1995**, *24*, 391.
(32) Pyykkö, P. *Angew. Chem., Int. Ed.* **2004**, *43*, 4412.
(33) Raize, O.; Argaman, Y.; Yannai, S. *Biotechnol. Bioeng.* **2004**, *87*, 451.
(34) Bachman, R. E.; Bodolosky-Bettis, S. A.; Glennon, S. C.; Sirchio, S. A. *J. Am. Chem. Soc.* **2000**, *122*, 7146.
(35) Assefa, Z.; McBurnett, B. G.; Staples, R. J.; Fackler, J. P.; Assmann, B.; Angermaier, K.; Schmidbaur, H. *Inorg. Chem.* **1995**, *34*, 75.
(36) Cha, S.-H.; Kim, J.-U.; Kim, K.-H.; Lee, J.-C. *Chem. Mater.* **2007**, *19*, 6297.
(37) Schneider, J.; Lee, Y.-A.; Perez, J.; Brennessel, W. W.; Flaschenriem, C.; Eisenberg, R. *Inorg. Chem.* **2008**, *47*, 957.
(38) Che, C.-M.; Kwong, H.-L.; Poon, C.-K.; Yam, V. W.-W. *J. Chem. Soc., Dalton Trans.* **1990**, 3215.
(39) He, X.; Yam, V. W.-W. *Coord. Chem. Rev.* **2011**, *255*, 2111.
(40) Yam, V. W.-W.; Kam-Wing, Lo, K. *Chem. Soc. Rev.* **1999**, *28*, 323.
(41) Ito, H.; Saito, T.; Oshima, N.; Kitamura, N.; Ishizaka, S.; Hinatsu, Y.; Wakeshima, M.; Kato, M.; Tsuge, K.; Sawamura, M. *J. Am. Chem. Soc.* **2008**, *130*, 10044.
(42) Valeur, B. *Molecular Fluorescence: Principles and Applications*; Wiley–VCH: Weinheim, Germany, 2002.
(43) Schmidbaur, H. *Gold Bull.* **1990**, *23*, 11.
(44) Vickery, J. C.; Olmstead, M. M.; Fung, E. Y.; Balch, A. L. *Angew. Chem., Int. Ed.* **1997**, *36*, 1179.
(45) Häkkinen, H.; Walter, M.; Grönbeck, H. *J. Phys. Chem. B* **2006**, *110*, 9927.
(46) Qian, H.; Jin, R. *Nano Lett.* **2009**, *9*, 4083.
(47) Levi-Kalisman, Y.; Jadzinsky, P. D.; Kalisman, N.; Tsunoyama, H.; Tsukuda, T.; Bushnell, D. A.; Kornberg, R. D. *J. Am. Chem. Soc.* **2011**, *133*, 2976.
(48) Qian, H.; Eckenhoff, W. T.; Zhu, Y.; Pintauer, T.; Jin, R. *J. Am. Chem. Soc.* **2010**, *132*, 8280.
(49) Jadzinsky, P. D.; Calero, G.; Ackerson, C. J.; Bushnell, D. A.; Kornberg, R. D. *Science* **2007**, *318*, 430.
(50) Zhu, M.; Aikens, C. M.; Hollander, F. J.; Schatz, G. C.; Jin, R. *J. Am. Chem. Soc.* **2008**, *130*, 5883.
(51) Simpson, C. A.; Farrow, C. L.; Tian, P.; Billinge, S. J. L.; Huffman, B. J.; Harkness, K. M.; Cliffel, D. E. *Inorg. Chem.* **2010**, *49*, 10858.
(52) Shaw, C. F. *Chem. Rev.* **1999**, *99*, 2589.
(53) Tracy, J. B.; Crowe, M. C.; Parker, J. F.; Hampe, O.; Fields-Zinna, C. A.; Dass, A.; Murray, R. W. *J. Am. Chem. Soc.* **2007**, *129*, 16209.
(54) Tracy, J. B.; Kalyuzhny, G.; Crowe, M. C.; Balasubramanian, R.; Choi, J.-P.; Murray, R. W. *J. Am. Chem. Soc.* **2007**, *129*, 6706.
(55) Brack, M. *Rev. Mod. Phys.* **1993**, *65*, 677.
(56) Hakkinen, H. *Nat. Chem.* **2012**, *4*, 443.